

HASAN, M.J. and KIM, J. 2020. Deep convolutional neural network with 2D spectral energy maps for fault diagnosis of gearboxes under variable speed. In *Djeddi, C., Jamil, A. and Siddiqi, I. (eds.) Pattern recognition and artificial intelligence: proceedings of the 3rd Mediterranean conference on pattern recognition and artificial intelligence (MedPRAI 2019), 22-23 December 2019, Istanbul, Turkey*. Communications in computer and information science (CCIS), 1144. Cham: Springer [online], pages 106-117. Available from: https://doi.org/10.1007/978-3-030-37548-5_9

Deep convolutional neural network with 2D spectral energy maps for fault diagnosis of gearboxes under variable speed.

HASAN, M.J. and KIM, J.

2020

This version of the contribution has been accepted for publication, after peer review (when applicable) but is not the Version of Record and does not reflect post-acceptance improvements, or any corrections. The Version of Record is available online at: https://doi.org/10.1007/978-3-030-37548-5_9. Use of this Accepted Version is subject to the publisher's [Accepted Manuscript terms of use](#).

Deep Convolutional Neural Network with 2D Spectral Energy Maps for Fault Diagnosis of Gearboxes Under Variable Speed

Md Junayed Hasan and Jongmyon Kim

Department of Electrical and Computer Engineering, University of Ulsan,
Ulsan, South Korea

junhasan@gmail.com, jmkim07@ulsan.ac.kr

Abstract. For industrial safety, correct classification of gearbox fault conditions is necessary. One of the most crucial tasks in data-driven fault diagnosis is determining the best set of features by analyzing the statistical parameters of the signals. However, under variable speed conditions, these statistical parameters are incapable of uncovering the dynamic characteristics of different fault conditions of gearboxes. Later, several deep learning algorithms are used to improve the performance of the feature selection process, but domain knowledge expertise is still necessary. In this paper, a combination domain knowledge analysis and a deep neural network is proposed. By using the input acoustic emission (AE) signal, a two-dimensional spectrum energy map (2D AE-SEM) is created to form an identical fault pattern for various speed conditions of gearboxes. Then, a deep convolutional neural network (DCNN) is proposed to investigate the detailed structure of the 2D input for final fault classification. This 2D AE-SEM offers a graphical depiction of acoustic emission spectral characteristics. Our proposed system offers vigorous and dynamic classification performance through the proposed DCNN with a high diagnostic fault classification accuracy of 96.37% in all considered scenarios.

Keywords: Gearbox safety · Fault diagnosis · Convolutional neural network

1 Introduction

Gearbox fault diagnosis is a substantial issue regarding the safety and excellence of various apparatuses in many industries. Specifically, gearbox fault diagnosis is featured in many different mechanical schemes, including wind turbines, cars, gas turbines, and helicopters [1–3]. Because they function in tough atmospheres, gearboxes habitually encounter gear tooth pitting and root breaking issues [4]. Several of these disasters can cause severe damage to the completely automated motorized structure, resulting in large economic losses and even the loss of human life. An enhanced cost-effective fault identification approach for gearboxes under invariant speed conditions (revolutions per minutes (RMPs)) can ensure functioning dependability and lessen protection expenditures.

Data driven fault diagnosis is accomplished by accumulating data (i.e., vibration signals (VS) and acoustic emission signals (AE)), comprising an essential part of investigations structured over the previous decades [5–8]. Such research confirms that fault condition diagnosis can decrease preservation costs by improving the consistency of the machinery [6, 9, 10]. AE signals can secure fundamental information from low-energy signals [11–14]. This establishes AE signals as an effective method for data-driven fault diagnosis tactics over vibration analysis (VA). This analysis suggests an AE-based fault identification methodology for gearboxes. Several studies (i.e., short term fourier transform [15], wavelet analysis [16]) tried to prove the domain based solution for fault classification by analyzing the extracted features from signals, but due to the inappropriate time-window adjustment, and inability to capture the high frequency resolutions at high frequencies; the main purpose is not solved in a robust manner.

This work mainly addresses two limitations for gearbox fault diagnosis: a) the necessity of domain level expertise for designing the best feature set for different fault conditions from statistical parameters under variable speed conditions, and b) the necessity of a deep dynamic algorithm (DDA) to investigate automated feature extraction in a reliable way to ensure industrial safety. The main focus of the proposed approach is to create a bridge between these two limitations using a singular-as-a-whole standalone algorithm. The proposed two-dimensional acoustic emission spectral energy map (2D AE-SEM) analyzes the root mean square (RMS) frequency distribution of individual signals to create an identical fault pattern under variable speed conditions. The energy density of this pattern increases incrementally with speed [5]. To capture the core fault pattern of the striking energies of this 2D AE-SEM from different speeds, a five-layer deep convolutional neural network (DCNN) is proposed. To establish the robustness of the proposed approach, various state-of-the-art algorithms (multiclass support vector machine + neural network using the statistical parameters [17] and spectral average + k-nearest neighbor algorithm (KNN) [18]) are considered for final comparisons.

The major contributions of the 2D AE-SEM + DCNN proposed in this work can be summarized as follows.

- (1) We present a unique 2D AE-SEM-based fault pattern visualization for various speeds for gearboxes to investigate the potential of AE signals.
- (2) This 2D AE-SEM is used as an input to the proposed five-layer deep convolutional neural network (DCNN) for fault classification in a speed invariant way. The proposed DCNN analyzes the input image pattern to discover the true feature information for final fault classification. Under different RPMs, experiments were used to validate our method by comparing with several state-of-the-art algorithms. The main purpose of using DCNN is to automatically distinguish the patterns for classifying different cracks.

The remaining part of our paper is organized as follows. Section 2 defines the details of the proposed methodology, including the gearbox data acquisition testbed. Section 3 describes the experimental result analysis to establish the robustness and dynamic attitude of the proposed algorithm. Finally, conclusions are drawn in Sect. 4.

2 Methodology

The proposed method consists mainly of three major sections. Data collection from an experimental testbed, forming a 2D AE Spectral Energy Map (2D AE-SEM), and the Deep Convolutional Neural Network (DCNN). The raw AE signal is collected from the AE sensors of the bearing housing end from two channels. Then, the AE signal is used to form the 2D AE-SEM as an input for the DCNN. The whole process is illustrated in Fig. 1.

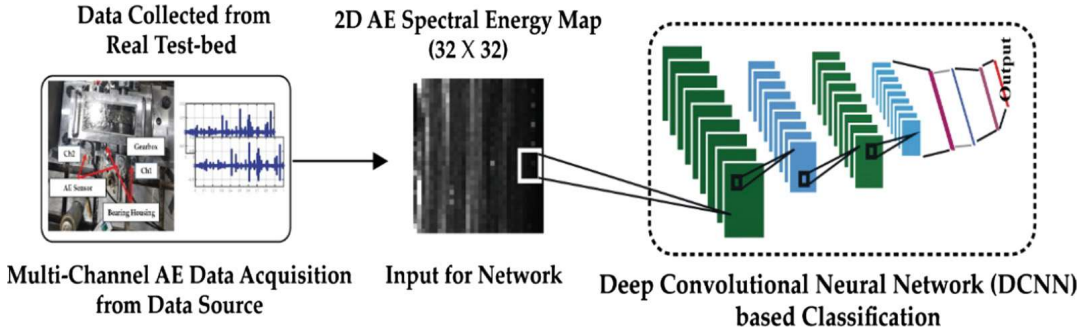


Fig. 1. The proposed 2D AE SEM + DCNN based gearbox health state classification approach.

2.1 Data Acquisition

In this experiment, we considered a simple gearbox with a gear ratio of 1.52:1. In the experimental testbed, two shafts are connected, specifically non-drive-end-shaft (NDS) and drive-end-shaft (DS). A three-phase induction motor is connected along with a displacement transducer at three different revolutions per minutes (RPM) (i.e., 300, 600, and 900 RPM) at the DS. The bearing house is attached to the motor shaft through the gearbox. At the NDS, a $WS\alpha$ AE [19] sensor is placed over the bearing house in the shaft [5, 20]. AE signals are collected through the AE sensor at a sampling rate of 100,000 Hz using a PCI-2 [21] system. The experimental testbed is illustrated in Fig. 2. The specification of the gears used in this data acquisition system is given in Table 1.

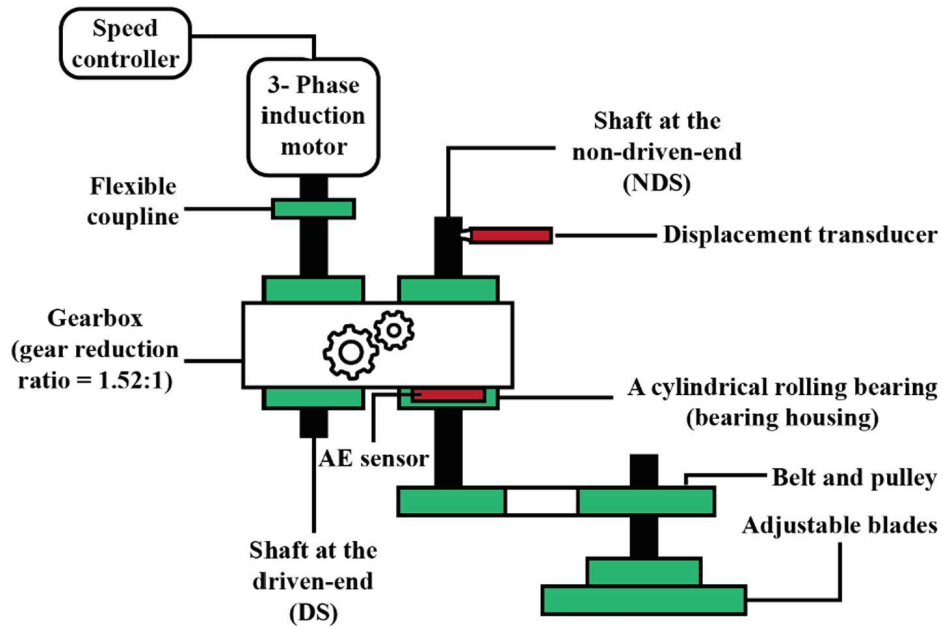





Fig. 2. Schematic of the experimental testbed for gearbox fault identification.

Table 1. Detailed gear specifications.

Gear Specification	Number of drive shaft teeth: 25
	Number of driven coaxial teeth: 38
	Tooth length: 9 mm

To create the different health conditions, an artificial defect is created on the shaft gear. The specifications of the faulty health conditions of the driven shaft gear are given in Table 2.

Table 2. Specifications of the defective coaxial driven shaft gear.

Health Condition	Picture	Defect Length (mm)
10% Crack (C10)		0.9
20% Crack (C20)		1.8
30% Crack (C30)		2.7

2.2 2D Acoustic Emission Spectral Energy Map (2D AE-SEM)

After collecting the raw AE signal, the unwanted noises are removed through a white-noise cancellation process. After that, the Fast Fourier transformation (FFT) is calculated to obtain the positive frequency response from the input signal. The AE spectrum has 50×10^4 positive frequency components, which is not a suitable input to DCNN. Therefore, the considered positive AE spectrum is divided into several frequency bins. From each bin, the root mean square (RMS) frequency is calculated. These RMS frequency values were used to create the 1D AE – Spectral Energy Map (1D AE-SEM). Finally, the 1D AE-SEM of length 1024 is reformed to create a 2D AE-SEM with a size of 32×32 . This 2D AE-SEM creates identical patterns for different health conditions with regard to invariant speed scenarios. The 2D AE-SEM has reasonable dimensions to be used as an input to the proposed DCNN for final classification [5]. The total process of forming the 2D AE-SEM is given as a flowchart in Fig. 3.

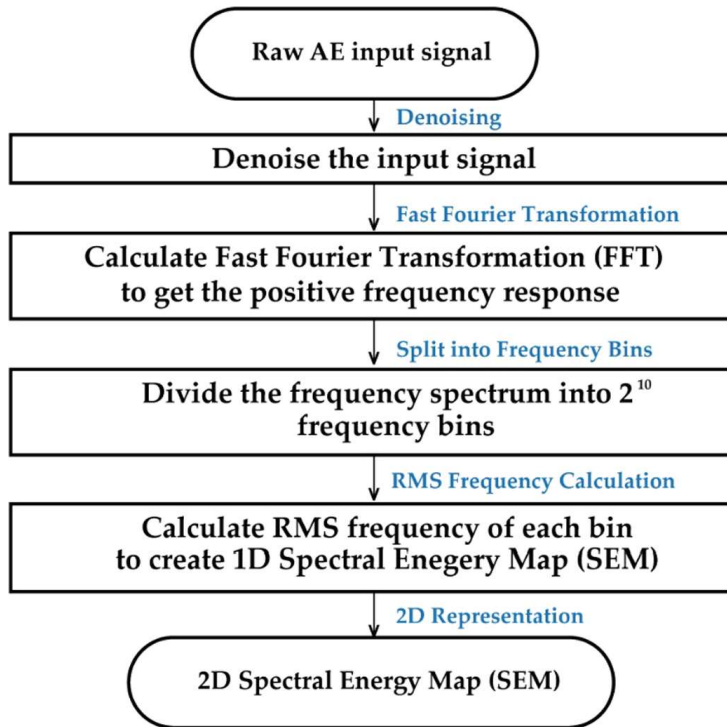


Fig. 3. Overall process of creating a 2D AE-SEM.

2.3 Deep Convolutional Neural Network (DCNN) for Fault Classification

A Deep Convolutional Neural Network (DCNN) is one of the most efficient supervised machine learning approaches [22]. In our work, since we are considering 2D AE-SEM, we used the DCNN to uncover the details of the 2D input. In DCNN, if the input data is $X = [x_1, x_2, \dots, x_m]$, then the total training sample size is m . Furthermore, the output vector is $Y = [y_1, y_2, \dots, y_m]$, which is supplementary to X . If P layers represent a

CNN, then each layer in the DCNN has F^p elements, which are utilized in convolution and max pooling [23]. The sigmoid activation function $\sigma(\cdot)$ is considered.

The proposed DCNN architecture is illustrated in Fig. 4. The detailed specifications of the proposed DCNN are listed in Table 3.

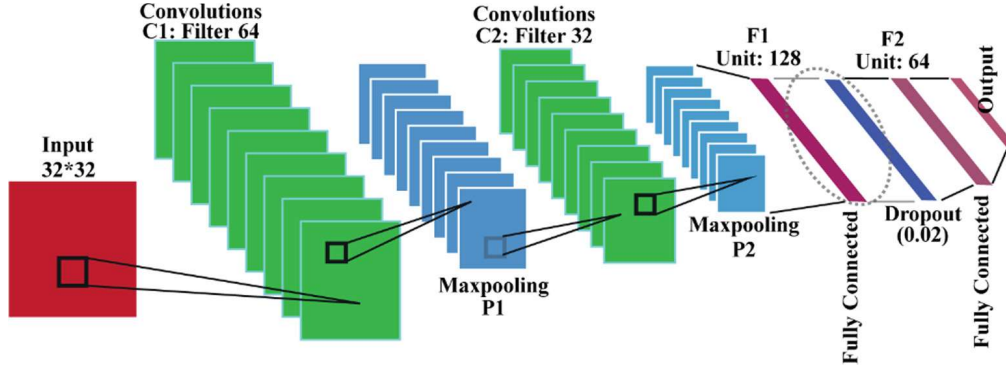


Fig. 4. The proposed structure of the DCNN.

Table 3. The dimensions of the Deep Convolutional Neural Network (DCNN)

Layers	Parameters	Observations	Height	Width	Depth	Trainable
Input		Preprocessed signals	32	32	3	
Conv1	Kernel	Filter	6	6		Yes
	Padding	Zero				
	Depth	Filter number			64	
MaxPool1	Kernel	Filter	3	3		No
	Padding	Zero				
Conv2	Kernel	Filter	3	3		Yes
	Padding	Zero				
	Depth	Filter number			32	
MaxPool2	Kernel	Filter	3	3		No
	Padding	Zero				
FC1	Nodes	Flatten as 1D	128			Yes
Dropout	Output		128			No
FC2	Nodes	Flatten as 1D	64			
Softmax	Nodes	Flatten into 1D	3			Classify

3 Result and Discussion

3.1 Dataset Description

For in-depth assessment of the proposed (2D AE-SEM + DCNN) fault classification approach, the following methods were used. The first method is the 2D AE-SEM-based

invariant gearbox health state visualization. The second is DCNN-based RPM invariant performance analysis of health state classification and extensive comparisons with some state of art methods (i.e., multiclass support vector machine + neural network using the statistical parameters [17], spectral average + k-nearest neighbor algorithm (KNN) [18]). The standard AE dataset of gearbox crack faults from the experimental testbed is used throughout the whole experiment. We have used three different RPMs (300, 600, and 900) and recorded 100 signals of one second for each health type (e.g., C10, C20 and C30) at each RPM. The specifics of the collected dataset are presented in Table 4.

Table 4. Measured fault conditions for different datasets

	Health type	Shaft speed (rpm)	Sampling frequency (Hz)
Dataset 1	10% Crack (C10)	300	100,000
	20% Crack (C20)	300	
	30% Crack (C30)	300	
Dataset 2	10% Crack (C10)	600	
	20% Crack (C20)	600	
	30% Crack (C30)	600	
Dataset 3	10% Crack (C10)	900	
	20% Crack (C20)	900	
	30% Crack (C30)	900	

3.2 Analysis of the 2D Acoustic Emission Spectral Energy Map

According to the previous discussion, the main reasons for constructing the 2D AE-SEM are (a) to create an invariant scenario for different RPMs under different health conditions, and (b) to deliver the benefits of 2D image structures to the DCNN with a minimum visibility of similar patterns.

Figure 5 exhibits the 2D AE-SEMs for different health conditions. For each RPM, the images of different health conditions show some identical information. From Fig. 5 (a), we can observe that for the C10 health condition, the striking energy of the RMS frequency in the 2D AE-SEM maintains some matching patterns. When the RPM increased, the energy striking density also increased. Thus, the amount of white strikes increases. From Fig. 5(b) and (c), we observe a similar situation for health states C20 and C30 respectively. Due to high RPM, the density of the striking energy increases. Thus, the similarity of these patterns has been carefully uncovered and handled through the proposed DCNN for the final classification analysis.

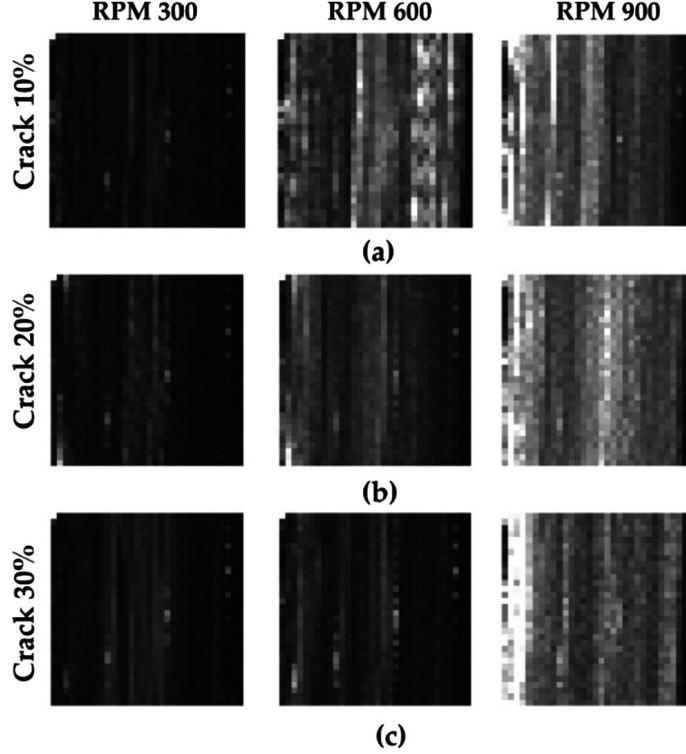


Fig. 5. From all the working conditions given in Table 4, the 2D AE-SEMs for different health conditions are displayed, i.e., (a) C10 (b) C20, and (c) C30 for different RPMs.

3.3 Diagnostic Performance of a Deep Convolutional Neural Network

To validate the proposed approach, we considered three different datasets (described in Table 4). These datasets contain different speeds with similar health conditions. The rpm invariance of this method is confirmed by examining three separate scenarios. In the first scenario, dataset 1 is used for training the DCNN, and datasets 2 and 3 are used for classification tests. In the second scenario, dataset 2 is used for training, and datasets 1 and 2 are used for testing. Similarly, in scenario 3, dataset 3 is used for training while the other two datasets are utilized for testing and classification. For evaluation of the analytical performance, we considered the F1 score as the basic classification performance matrix (F1), average classification accuracy (AC), and overall classification accuracy (OC) [5, 24]. The main reason for considering the F1 score for classification accuracy measurement is to balance between the Recall and Precision scores.

$$F1 = \frac{T_{positive}}{T_{positive} + \frac{F_{negative} + F_{positive}}{2}} \times 100(\%) \quad (1)$$

Here, $T_{positive}$ is the number of correctly classified samples from a particular class and $F_{negative}$ is the number of incorrectly classified sample from a particular class. The final result is calculated as a percentage. After computing the final F1 score of a particular health condition, the average classification accuracy (AC) is measured following Eq. (2).

$$AC = \frac{\sum F1}{\sum T_{Classes}} \quad (2)$$

Finally, the overall classification accuracy, based on a particular scenario (OC), is obtained as Eq. (3).

$$OC = \frac{\sum TD_{AC}}{\sum T_{Scenario}} \quad (3)$$

Here, $\sum TD_{AC}$ defines the total of the CA test dataset, and $\sum T_{Scenario}$ describes the total number of test datasets existing in a discrete scenario.

Table 5 records the details of the analytical accomplishment of the proposed 2D AE-SEM + DCNN based approach. In Table 4, we see an interesting trend. From Figs. 5(a), (b), and (c), we see that the striking energy rises while RPM increases. Dataset 1 represents the lowest RPM here. Thus, from the 2D AE-SEM, we observe that rather than dataset 1, the patterns are more densely repeated in datasets 2 and 3. For scenario 1 in Table 5, when the DCNN is trained with dataset 1, the OC becomes 94.62%. When we move to scenario 2, where the DCNN is trained with dataset 2, the OC increases to 96.99%. Finally, when the network is trained with dataset 3, the performance increases to its optimal value, which is 97.5%. This means that while there is a repetitive pattern, the network learns details much better for classification. The average classification accuracy is 96.37% at the end.

Table 5. Analytical implementation of the proposed model for various scenarios

Scenario	Training dataset	Test dataset	F1 (%)			CA (%)	OC (%)
			C10	C20	C30		
1	Dataset 1	Dataset 2	95.22	94.39	94.41	94.67	94.62
		Dataset 3	94.93	94.17	94.59	94.56	
2	Dataset 2	Dataset 3	96.41	95.39	95.37	97.72	96.99
		Dataset 1	96.29	96.71	95.74	96.25	
3	Dataset 3	Dataset 1	97.83	98.2	97.49	97.84	97.5
		Dataset 2	97.72	97.32	96.43	97.16	
Average						96.37	

For this experiment, we used 500 epochs for training and testing. While training the network for each scenario, we considered 80% of the data for training and 20% for validation from the training dataset. For performance evaluation, 8-fold cross-validation is used. While training the network for each scenario, the loss function Adam performed better than the stochastic gradient decent (sgd). Figure 6 shows the loss curve performance analysis (sgd vs. Adam) for dataset 1 and dataset 2 while training the DCNN for scenario 1 and scenario 2, respectively.

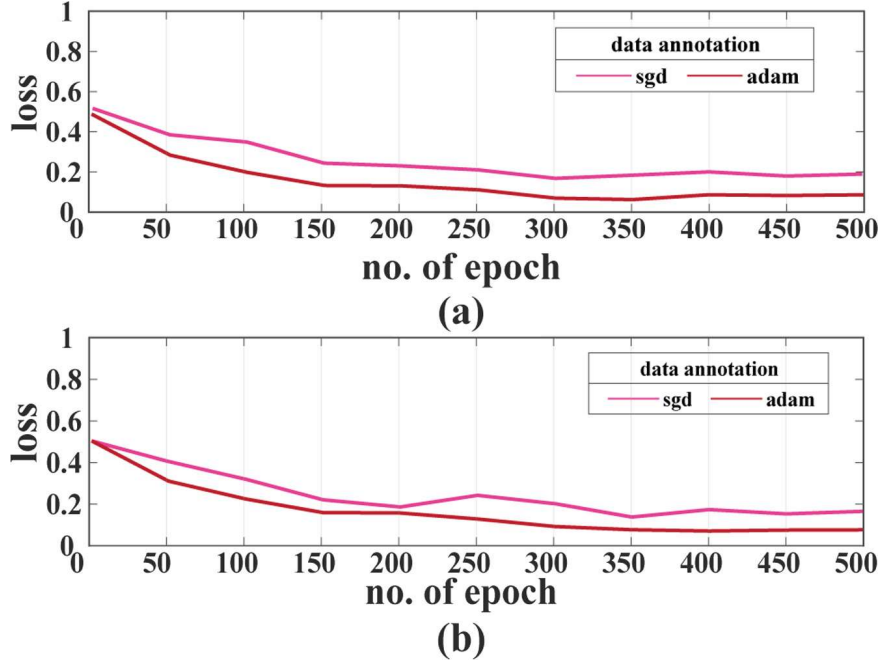


Fig. 6. Loss curve performance analysis while training the DCNN (sgd vs. Adam), (a) dataset 1 for scenario 1, and (b) dataset 2 for scenario 2.

3.4 Comparison Analysis

To demonstrate the robustness of the proposed approach, we made several comparisons with state-of-the-art approaches, i.e., the multiclass support vector machine + neural network using the statistical parameters [17] and the spectral average + k-nearest neighbor algorithm (KNN) [18]. The comparison of classification accuracy (F1 score (%) and the average classification accuracy (AC)) is described in Table 6. From Table 6, we see that our proposed approach outperformed these state of art approaches by at least 4.74% accuracy for each scenario. To ensure a fair comparison, similar settings for the training and testing data as given in Table 4 are used.

Table 6. Comparison analysis of different methods

Scenario	Method	F1 (%)			AC (%)	Improved (%)
		C10	C20	C30		
1	[17]	89.4	88.9	91.4	89.9	4.74
	[18]	48.52	47.22	47.9	47.88	46.76
	Proposed	95.08	94.28	94.5	94.64	–
2	[17]	89.91	87.2	88.6	88.57	8.42
	[18]	49.11	48.73	47.44	48.43	48.56
	Proposed	96.35	96.05	95.56	96.99	–
3	[17]	90.2	88.7	90.43	89.78	7.72
	[18]	48.37	47.39	48.27	48.01	49.49
	Proposed	97.78	97.76	96.96	97.5	–

4 Conclusion

This work proposed a two-dimensional acoustic emission spectral energy map (2D AE-SEM) with fault diagnosis based on a five-layer deep convolutional neural network (DCNN) for ensuring the safety and reliability of the gearbox, which is invariant to the shaft speed. In traditional approaches, consideration of the statistical parameters from signals and defect frequency analysis have several difficulties regarding premeditated differences in shaft speed. This study considered an invariant scenario for different fault conditions with respect to various RPMs by creating a 2D AE-SEM. The proposed DCNN utilized the 2D AE-SEM input structure for final fault condition analysis. The proposed method achieved an overall 96.37% classification accuracy. In addition, this work out-performed two state-of-the-art approaches with an overall improvement of at least 4.74%, and 46.76%, respectively, in the three considered scenarios.

Acknowledgements. This research was financially supported by the Ministry of Trade, Industry & Energy (MOTIE) of the Republic of Korea and Korea Institute for Advancement of Technology (KIAT) through the Encouragement Program for The Industries of Economic Cooperation Region (P0006123). This work was partly supported by the Korea Institute of Energy Technology Evaluation and Planning (KETEP) and the Ministry of Trade, Industry & Energy (MOTIE) of the Republic of Korea (No. 20172510102130)

References

1. Zhao, M., Kang, M., Tang, B., Pecht, M.: Deep residual networks with dynamically weighted wavelet coefficients for fault diagnosis of planetary gearboxes. *IEEE Trans. Ind. Electron.* **65**, 4290–4300 (2018)
2. Chen, X., Feng, Z.: Time-frequency demodulation analysis for gearbox fault diagnosis under nonstationary conditions. In: 2016 IEEE International Conference Prognostics and Health Management ICPHM 2016, pp. 1–6 (2016)
3. Du, Z., Chen, X., Zhang, H., Yan, R.: Sparse feature identification based on union of redundant dictionary for wind turbine gearbox fault diagnosis. *IEEE Trans. Ind. Electron.* **62**, 6594–6605 (2015)
4. Chaari, F., Fakhfakh, T., Haddar, M.: Dynamic analysis of a planetary gear failure caused by tooth pitting and cracking. *J. Fail. Anal. Prev.* **6**, 73–78 (2006)
5. Tra, V., Kim, J., Khan, S.A., Kim, J.-M.: bearing fault diagnosis under variable speed using convolutional neural networks and the stochastic diagonal Levenberg-Marquardt algorithm. *Sensors* **17**, 2834 (2017)
6. Sohaib, M., Kim, C.-H., Kim, J.-M.: A hybrid feature model and deep-learning-based bearing fault diagnosis. *Sensors*. **17**, 2876 (2017)
7. Zhao, S., Liang, L., Xu, G., Wang, J., Zhang, W.: Quantitative diagnosis of a spall-like fault of a rolling element bearing by empirical mode decomposition and the approximate entropy method. *Mech. Syst. Signal Process.* **40**, 154–177 (2013)
8. Yu, X., Ding, E., Chen, C., Liu, X., Li, L.: A novel characteristic frequency bands extraction method for automatic bearing fault diagnosis based on Hilbert Huang transform. *Sens. (Switzerland)*. **15**, 27869–27893 (2015)
9. Yin, S., Ding, S.X., Zhou, D.: Diagnosis and prognosis for complicated industrial systems - Part I. *IEEE Trans. Ind. Electron.* **63**, 2501–2505 (2016)

10. Yin, S., Ding, S.X., Zhou, D.: Diagnosis and prognosis for complicated industrial systems - Part II. *IEEE Trans. Ind. Electron.* **63**, 3201–3204 (2016)
11. Eftekharijad, B., Carrasco, M.R., Charnley, B., Mba, D.: The application of spectral kurtosis on acoustic emission and vibrations from a defective bearing. *Mech. Syst. Signal Process.* **25**, 266–284 (2011)
12. Widodo, A., et al.: Fault diagnosis of low speed bearing based on relevance vector machine and support vector machine. *Expert Syst. Appl.* **36**, 7252–7261 (2009)
13. Pandya, D.H., Upadhyay, S.H., Harsha, S.P.: Fault diagnosis of rolling element bearing with intrinsic mode function of acoustic emission data using APF-KNN. *Expert Syst. Appl.* **40**, 4137–4145 (2013)
14. Caesarendra, W., Kosasih, P.B., Tieu, A.K., Moodie, C.A.S., Choi, B.K.: Condition monitoring of naturally damaged slow speed slewing bearing based on ensemble empirical mode decomposition. *J. Mech. Sci. Technol.* **27**, 2253–2262 (2013)
15. Kim, B.S., Lee, S.H., Lee, M.G., Ni, J., Song, J.Y., Lee, C.W.: A comparative study on damage detection in speed-up and coast-down process of grinding spindle-typed rotor-bearing system. *J. Mater. Process. Tech.* **187–188**, 30–36 (2007)
16. Tahir, M.M., Khan, A.Q., Iqbal, N., Hussain, A., Badshah, S.: Enhancing fault classification accuracy of ball bearing using central tendency based time domain features. *IEEE Access* **5**, 72–83 (2017)
17. Jin, X., Zhao, M., Chow, T.W.S., Pecht, M.: Motor bearing fault diagnosis using trace ratio linear discriminant analysis. *IEEE Trans. Ind. Electron.* **61**, 2441–2451 (2014)
18. Del Campo, V., Ragni, D., Micallef, D., Diez, J., Simão Ferreira, C.J.: Vibration-based wind turbine planetary gearbox fault diagnosis using spectral averaging. *Wind Energy* **18**, 1875–1891 (2015)
19. Physicalacoustics – sensors. <https://www.physicalacoustics.com/by-product/sensors/WDI-AST-100-900-kHz-Wideband-Differential-AE-Sensor>
20. Islam, M.M.M., Myon, J.: Time–frequency envelope analysis-based sub-band selection and probabilistic support vector machines for multi-fault diagnosis of low-speed bearings. *J. Ambient Intell. Humaniz. Comput.* (2017). <https://doi.org/10.1007/s12652-017-0585-2>
21. Physicalacoustics - PCI 2. <https://www.physicalacoustics.com/by-product/pci-2/>
22. Malek, S., Melgani, F., Bazi, Y.: One-dimensional convolutional neural networks for spectroscopic signal regression. *J. Chemom.* **32**, 1–17 (2017)
23. Zhang, R., Tao, H., Wu, L., Guan, Y.: Transfer learning with neural networks for bearing fault diagnosis in changing working conditions. *IEEE Access* **5**, 14347–14357 (2017)
24. Hasan, M.J., Islam, M.M.M., Kim, J.M.: Acoustic spectral imaging and transfer learning for reliable bearing fault diagnosis under variable speed conditions. *Meas. J. Int. Meas. Confed.* **138**, 620–631 (2019)